Journal of Engineering Science and Technology
EURECA 2014 Special Issue January (2015) 19 - 31

COMPUTATIONAL STUDIES TO INVESTIGATE THE FUEL FEEDING POINT IN FLUIDIZED BED REACTOR

Y. C. YAN, X. Y. LIM*, W. RASHMI, C. H. LIM

School of Engineering, Taylor's University, Taylor's Lakeside Campus,
No. 1 Jalan Taylor's, 47500, Subang Jaya, Selangor DE, Malaysia
*Corresponding Author: xiaoyien.lim@taylors.edu.my

Abstract

As the world is concerned with the dependence of the transportation fuel on fossil fuels and its impact on greenhouse gas emissions, all regions in the world are driven to deploy bio-oil as the alternative transportation fuel. Pyrolysis, a process in which the organic materials undergo thermal degradation in the absence of oxygen, has shown great potential to be competitive with the conventional petroleum production in terms of economy and quality. With the advancement of computational fluid dynamics (CFD), it allows detailed analysis and optimization of a pyrolysis process to be carried out easily and thus indirectly minimizes all the expensive and time-consuming experiment. As different biomass species show varied physical and chemical properties, feeding point of the biomass in the fluidized bed reactor (FBR) requires careful consideration. This is because the feeding point will affect the conversion efficiency of the biomass, the heat transfer of the biomass particles and also the residence time in the reactor. In this paper, the influence of the fuel feeding point on the products' yield is investigated in a pyrolysis FBR using ANSYS Fluent 14.0 simulation. The biomass feeding point will be focused on 3 different zones – the freeboard, the splash zone and the dense bed. The reactor's dimension, boundary conditions and initial conditions are similar as described in the selected benchmark paper by Xue et al. (2012). Simulation result is compared with the result reported in the benchmark paper for validation. With the validated model, the effect of feeding point was studied and it is observed that for pure cellulose feedstock the optimum feeding point is at the dense bed zone and for red oak the optimum feeding point is at the splash zone. Overall, this study provides a fundamental understanding of the influence of the fuel feeding point on the products yield and reactor temperature distribution during the pyrolysis process in a FBR.

Keywords: CFD, Fluent, Fast Pyrolysis, Fluidized Bed Reactor.

Nomenclatures

C_p	Heat capacity
$\vec{g}$	Gravity vector
H	Heat transfer
I	Force interaction due to momentum
k	Kinetic constant
$\vec{q}$	Heat flux
R	Reaction rate
$\overline{\overline{S}}$	Stress tensor
t	Time
T	Temperature
$\vec{u}$	Velocity of solid or gas
X	Mass fraction

Greek Symbols

ρ	Density

Abbreviations

CFD	Computational fluid dynamics
FBR	Fluidized bed reactor
UDF	User-defined function

1. Introduction

Every year, many plants are grown vastly through photosynthesis and absorbing CO_2 from the atmosphere. After the plants are harvested and process, many agricultural wastes remain. These agricultural wastes are a source of biomass. As it can be grown within a few years, biomass derived from agricultural wastes have provided a large source of renewable bioenergy to the world. Due to increasing needs of renewable energy to replace fossil fuels, energy derived from biomass has become a promising alternative energy source. One type of conversion to extract energy from biomass is fast pyrolysis. Fast pyrolysis is a thermal conversion process to extract energy from biomass with the absence of O_2 and high heating rate [1]. In fast pyrolysis, biomass is broken down into smaller hydrocarbons which are usually classified into condensable tars and noncondensable gas (methane, hydrogen, CO_2, CO). The primary product from pyrolysis is bio-oil, due to its diverse usage as fuel [2]. Fast pyrolysis in the past two decades has led to the development of various types of reactor, including ablative, auger, entrained flow, vacuum, rotating cone, fluidized and circulating fluidized bed [3]. From the industrial perspective, FBR has shown great potential for tar production compared to other different reactors [4,5]. This is due to the fact that FBR offers high particle heating rates and excellent mass and heat transfer between phases, making it the superior choice for fast pyrolysis process [6,7].

Despite the advancement made in the pyrolysis route for bio-oil production, there are still some technical challenges, including measuring the flow of reacting dense gas-solid is both challenging and limited to today's measuring technique and knowledge to enable large-scale industrialization to take place [8]. With computational fluid dynamics (CFD), detailed analysis such optimum particle size

and temperature of a pyrolysis process could be achieved. CFD is considered the new "third approach" in the research field of fluid dynamics [9]. It allows the optimization of the operating conditions to be carried out in a simulated model, which indirectly minimizes the need to conduct expensive and time-consuming experimental testing [10]. The current computational power has made CFD an equivalent cohort with pure theory and pure experiment in the analysis and research of fluid dynamic challenges [11]. According to Fox [12] on CFD analysis of chemical reactors, the current CFD is capable to predict the material transport and chemical reactions in a plant-scale pyrolysis FBR which would result in much rapid development with lower cost. A few successful simulation works of fast pyrolysis on wood for bio-oil production has been studied [3,13].

The pyrolysis process in a FBR is a multiphase flow that consists of gas, solid, and gas-solid mixture flow that are mixed and reacting at the same time. Several models have been developed and the model developed by Lathouwers and Bellan [14] is considered to be one of the most comprehensive which utilizes the kinetic theory of granular flow to model the multiphase flow. Some other model incorporates user defined function (UDF) in an Euler-Lagrange approach in the modelling a single biomass particle in FBR [10]. In this paper, the multiphase flow is modelled using the Euler-Euler approach in which the solid sand and the solid biomass are both assumed to behave like a fluid. The objective of the current model is to simulate the fast pyrolysis in FBR using ANSYS Fluent 14.0. The fluidizing sand bed is incorporated with the commercial code via UDF written in C programming language. The further objective is to study the effect of the feeding point on the fast pyrolysis of biomass in the FBR focusing on pure cellulose and red oak feedstock.

2. Research Methodology

2.1. Model formulation

This research is a qualitative study on the effect of the biomass feeding point in pyrolysis FBR on the both temperature and the product yield. This simulation is modelled using ANSYS Fluent 14.0 on Dell Precision T7600 with Intel Xeon E5-2609 @2.40GHz processor and 16.0GB memory.

For the ease of modelling, each species that will participate in the pyrolysis process are assigned to an index that will be used in the kinetic model. The species index is given in Table 1 and the reaction rate of each species is tabulated in Table 2.

Table 1. Assignment of index for each species.

Index (*n*)	Species (phase)
1	Cellulose (s)
2	Hemicellulose (s)
3	Lignin (s)
4	Active Cellulose (s)
5	Active Hemicellulose (s)
6	Active Lignin (s)
7	Tar (g)
8	Gas (g)
9	Char (s)

Table 2. The reaction rate for each species.

Species(phase)	Reaction Rate, *R*
Cellulose(s)	$-\rho_{bio}X_1k_{1c}$
Hemicellulose(s)	$-\rho_{bio}X_2k_{1h}$
Lignin(s)	$-\rho_{bio}X_3k_{1l}$
Active Cellulose(s)	$\rho_{bio}X_1k_{1c} - \rho_{bio}X_4(k_{2c} + k_{3c})$
Active Hemicellulose(s)	$\rho_{bio}X_2k_{1h} - \rho_{bio}X_5(k_{2h} + k_{3h})$
Active Lignin(s)	$\rho_{bio}X_3k_{1l} - \rho_{bio}X_6(k_{2l} + k_{3l})$
Tar(g)	$\rho_{bio}X_4k_{2c} + \rho_{bio}X_5k_{2h} + \rho_{bio}X_6k_{2l} - m_gX_7k_4$
Gas(g)	$\rho_{bio}X_4k_{3c}(1 - Y_c) + \rho_{bio}X_5k_{3h}(1 - Y_h) + \rho_{bio}X_6k_{3l}(1 - Y_l) + m_gX_7k_4$
Char(s)	$\rho_{bio}X_4k_{3c}Y_c + \rho_{bio}X_5k_{3h}Y_h + \rho_{bio}X_6k_{3l}Y_l$

*bio=biomass; g=gas; c= cellulose; h=hemicellulose; l=lignin

In this model, three governing equations, which are the continuity equations, momentum equations, and energy equations, are solved during the simulation [9]. The model consist of gas phase (which are the products from the pyrolysis of biomass) and solid phase (which is biomass), each governing equations will be solved in a continuum for each phase where ρ is the density of the gas or solid, $\vec{u}$ is the velocity of the solid or gas, and R is the mass transfer due to reaction from solid to gas or vice versa. The R expressions are listed in Table 2.

Gas Phase: $\frac{\partial \rho_g}{\partial t} + \nabla.\left(\rho_g \vec{u}_g\right) = R_g$ (1)

Solid Phase: $\frac{\partial \rho_s}{\partial t} + \nabla.\left(\rho_s \vec{u}_s\right) = R_s$ (2)

The momentum equations for the pyrolysis of biomass in FBR are as follows [8, 9]; where $\overline{\overline{S}}$ is the stress tensor for gas phase or the solid phase, I represent the force interaction due to momentum transfer either between the gas and solid or the solid and solid, and $\vec{g}$ is the gravity vector.

Gas Phase: $\frac{\partial \rho_g \vec{u}_g}{\partial t} + \nabla.\left(\rho_g \vec{u}_g \vec{u}_g\right) = \nabla.\overline{\overline{S}}_g + \sum \vec{I}_{gs} + \rho_g \vec{g}$ (3)

Solid Phase: $\frac{\partial \rho_s \vec{u}_s}{\partial t} + \nabla.\left(\rho_s \vec{u}_s \vec{u}_s\right) = \nabla.\overline{\overline{S}}_s + \vec{I}_{gs} - \sum \vec{I}_{ss} + \rho_s \vec{g}$ (4)

The energy equations for the pyrolysis of biomass in FBR are as follows, where C_p is the heat capacity of the gas phase or the solid phase, T is the temperature of the gas phase or solid phase, $\vec{q}$ is the heat flux of the gas phase or the solid phase, H_{gs} is the heat transfer between the solid phase and gas phase, and ΔH_r is the heat of reaction for gas phase or the solid phase. In Eq. (5), the $H_{wall}\left(T_{wall} - T_g\right)$ accounts for the heat transfers between the gas phase and the wall.

Gas Phase: $\rho_g C_{pg}\left(\frac{\partial T_g}{\partial t} + \vec{u}_g.\nabla T_g\right) = \nabla.\vec{q}_g - \sum H_{gs} - \Delta H_{rg} + H_{wall}\left(T_{wall} - T_g\right)$ (5)

Solid Phase: $\rho_s C_{ps}\left(\frac{\partial T_s}{\partial t} + \vec{u}_s.\nabla T_s\right) = \nabla.\vec{q}_s - \sum H_{gs} - \Delta H_{rs}$ (6)

2.2. Multiphase model

In order to model the particle-particle heat transfer and collision in the FBR, it is important to select a multiphase model that gives the best representation of the flow. In this paper, the multiphase model using the Euler-Euler approach is proposed to model the FBR. Under this approach, the gas phase and the particle phase are considered to be a continuum that is interpenetrating each other [15]. It utilizes the conservation of each phase that relates by the application of kinetic theory in the case of granular flow in FBR [16]. As the flow inside the FBR consist of fluid-solid flow (the granular flow) and the fluid-fluid flow (the non-granular flow), ANSYS [15] and Mellin et al. [17]. Mellin et al. recommend the implementation of Eulerian model. This model permits the modelling of multiple separated interacting phases by using the formulation of constitutive equations, making the simulation requires less computational time [16-18]. According to Xue et al. [8], the implementation of the Eulerian model takes into account the inconsistent density of the biomass due to the chemical reaction in the FBR. This allows the freshly fed biomass, partially converted biomass, and fully converted biomass to reside in the biomass phase.

The Eulerian multiphase model requires UDF to model the sand bed in the FBR. In this research, the UDF of the Eulerian model is constructed based on the work conducted by Kuipers, Prins and Swaaij [19] on numerical calculation in a gas FBR. As the said research focuses on the interaction of heat transfer in the FBR, it can be related to this research. Hence, the UDF in this research used the same numerical calculation as in the said research above.

2.3. Viscous model

The work done by Loha, Chattopadhyay and Chatterjee [20] on FBR shows that there is no obvious difference in flow prediction in the modelling of the FBR with or without turbulence model, when compared to the experimental results. In fact, the research done by Hamidipour, Chen and Larachi [21] shows that the laminar model has better performance in predicting the flow in FBR compared to turbulence model. As a conclusion, laminar model is selected as the viscous model to simulate the flow inside the FBR in this research.

2.4. Chemical kinetics model

Fundamentally, the kinetic model of the decomposition of biomass obeys the Arrhenius rate expression [22]. The kinetic mechanism used in this study to model the biomass decomposition is the multi-stage semiglobal kinetic scheme as illustrated in Fig. 1 [23-25]. The decomposition rate of a biomass is the sum of the decomposition of cellulose, hemicellulose and lignin. All the decomposition rates are in first-order. In this study, two different feedstock is used; the pure cellulose and red oak. The red oak consists of 41wt% cellulose, 32wt% hemicellulose and 27wt% lignin. The kinetic parameters of each biomass component are based on the experimental values from literature listed in Table 3.

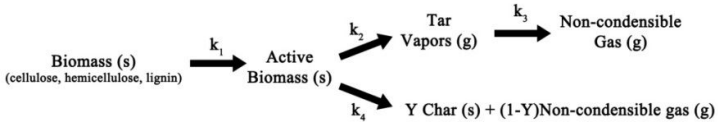

Fig. 1. The global kinetic scheme for cellulose, hemicellulose, and lignin.

Table 3. Kinetic parameters for the biomass components..

Reactions	Y of k_3	A (s^{-1})	E (kJ/kmol)
Cellulose [23]			
k_1	-	2.80×10^{19}	242.4×10^{3}
k_2	-	3.28×10^{14}	196.5×10^{3}
k_3	0.35	1.30×10^{10}	150.5×10^{3}
Hemicellulose [26]			
k_1	-	2.10×10^{16}	186.7×10^{3}
k_2	-	8.75×10^{15}	202.4×10^{3}
k_3	0.60	2.60×10^{11}	145.7×10^{3}
Lignin [26]			
k_1	-	9.60×10^{8}	107.6×10^{3}
k_2	-	1.50×10^{9}	143.8×10^{3}
k_3	0.75	2.60×10^{6}	111.4×10^{3}
Tar [27]			
k_4	-	2.6×10^{6}	108.0×10^{3}

2.5. Computational domain and boundary conditions

The 2-D model is solved using pressure-based ANSYS Fluent 14.0 as shown in Fig. 2. The isothermal wall is defined with a constant temperature of 800K whereas the remaining reactor's wall is defined as adiabatic wall. The inlet for the biomass is located on the left wall with a height of 0.73cm and the bottom of the inlet is 1.335cm above the bottom of the FBR. The biomass is fed into the FBR at 2.667×10^{-5} kg/s with an initial temperature of 300 K. The reactor operates at atmospheric pressure. Pure nitrogen gas with an initial temperature of 773 K is flowed into the reactor with a superficial velocity of 0.36 m/s. The sand bed is defined with an initial temperature of 773 K and a volume fraction of 0.59 with a particle diameter of 0.052cm. The computational domain and boundary conditions stated above are consistent with the benchmark paper by Xue et al. [8].

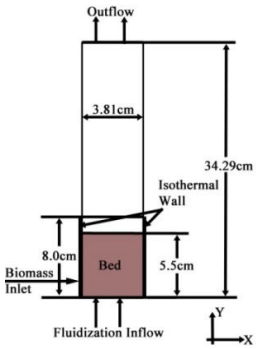

Fig. 2. The computational domain of the fluidized bed in this study.

The model consists of three phases; the first phase comprises of the nitrogen, tar vapour and non-condensible gas, the second phase is the inert sand bed, and the third phase consists of the biomass components. All simulation is run up to 100s of physical time using parallel runs on Dell Precision T7600.

2.6. Mesh dependency study

In order to ensure that the number of cells or the refinement of the mesh does not affect the accuracy of the result, the mesh dependency study is conducted by simulating a fluid flow in the FBR on different mesh refinement. In this paper, only the flow of nitrogen is simulated in FBR on three different mesh refinements (750, 1750 and 2660 elements). This is to determine the deviation between mesh refinement and whether the deviation is acceptable.

By analyzing the coefficient of variance, all three mesh refinement generated can be used for simulation without compromising the simulation results. Hence, with reference to the mesh refinement used in the benchmark paper, the 2660 number of elements is selected for this research in order to ensure the accuracy of the simulation result. Even though the number of cells is higher, the capability of the computer used in this research is exceeding that used in the benchmark paper. Therefore, it is justified to increase the number of cells to ensure the accuracy of the simulation result. As a conclusion, the number of cells in the model used in this research is 2660.

3. Validation

Model validation is crucial to ensure the simulation results are close to the reality. The simulation key results are compared and validated with the experimental result conducted by Xue et al. [8] which are shown in Table 4. The yields of the products are obtained through the surface integral report across the reactor's outlet.

Table 4. Comparison between the product yields (wt%) and FBR outlet temperature of pure cellulose and red oak in simulation and experiment [8].

Approach	Tar	Non-condensible Gas	Char	Outlet Temperature (K)
		Pure Cellulose		
Simulation	87.9	15.3	1.8	790.98
Experimental	82.1	12.4	2.2	773.15
		Red Oak		
Simulation	75.2	23.3	9.0	782.45
Experimental	71.7±1.4	20.5±1.3	13.0±1.5	773.15

It is important to first validate the simulation model using pure cellulose as the kinetic scheme described in Fig. 1 is based on cellulose and are superimposed on the remaining biomass components. The predicted results for pure cellulose, are in a good agreement with the experimental results quantitatively. The yield of tar (87.9%) is over-predicted, whereas the yield of the non-condensible gas (15.3%) is over-predicted. The prediction of char is in a very good agreement with a deviation of 0.4%. In this model, the biomass components are assumed to be spherical and experience no volume shrinkage during the pyrolysis [16]. This would affect the density change of the biomass during the reaction and over-estimated the biomass loss. The over-estimation of biomass loss would lead to residual in the simulation, causing formation of bio-gas to increase. Additionally, in this simulation, simplification was made such that the bio-gas is considered to be only methane. This simplification was made to enable a higher simulation performance and from the research on biomass pyrolysis, methane gas made up most of the bio-gas and is considered as a dominant component in this simulation

[28]. As such, the molecular weight of the bio-gas was assumed to be equal to the molecular weight of methane gas.

The red oak simulation on the other hand, shows a higher tar yield (75.2%) than the experimental result (71.7%). This is supported by the fact that the pyrolysis of lignin and hemicellulose is highly exothermic; hence, supplying more energy for the conversion of biomass to tar [1]. The biomass components in this simulation are considered to have similar physical density; hence, the prediction in bio-oil is almost similar to the prediction in the pure cellulose validation. The prediction of bio-gas yield (23.3%) is slightly higher than the experimental result (20.5%), this is expected from the simulation result shown in the over-prediction of the bio-gas in the validation of the pure cellulose. The presence of hemicellulose is also influencing the increase the yield of bio-gas [29]. Additionally, the bio-gas and bio-oil produced is assumed to escape the biomass immediately and are not trapped within the pore of the biomass or char particles. The predicted char yield is slightly lower (9.0%) than the experimental result (13.0%); however, it has a higher deviation compared to the validation of pure cellulose due to the presence of lignin in red oak [30].

As for the outlet temperature, the simulation result has the tendency to over-predict. This is due to the assumption made in the simulated model that no energy is loss from the reactor's adiabatic wall. Nevertheless, the deviation of the outlet temperature from the simulated model and the experimental results are less than 2.3%, which is within acceptable range for a simulated model.

4. Results and Discussion

In this research, four different feed-points as illustrated in Fig. 3 is investigated the using the validated CFD model. Table 5 consists of the exact location of the feed-points. Each feed-point is 0.73cm in diameter and the locations described in Table 5 are from the centre of the feed-point to the inflow boundary.

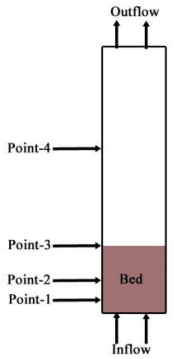

Fig. 3. The illustration of the feed-point study.

Table 5. The exact location of the feed-point in the fluidized bed model.

Feed-point Location	Point-1	Point-2	Point-3	Point-4
From the Inflow (cm)	1.7	2.4	5.5	19.9

4.1. Pure cellulose

In the investigation of fuel feeding point, pure cellulose is used as the feedstock first as the kinetic model is based on cellulose, and is superimposed on the remaining biomass components. Table 6 shows the collection of simulation data at the different feeding point for the simulated pyrolysis of pure cellulose.

From the results shown in Table 6, as the distance of the feeding point from the bottom of the sand bed increases, the yield of bio-oil decreases. In an ideal case, the biomass residence time should be larger than the total reaction time [31]. This justified that when the feeding point approaches the exit of the reactor, the residence time of biomass decreases presumably because the biomass are retained in the FBR for a shorter time, thus the pure cellulose decompose to a smaller extent. It is observed that at point-1 and point-2, the product yield is almost similar and this suggests that the change in residence time between these two points is very small to affect the product yield. However, at point-3, the bubbling surface of the sand bed greatly affected product yield as it was unable to retain the biomass component in the bed. Fairly similar bio-gas yield is observed at point-1, point-2 and point-3 because the conversion of bio-oil to bio-gas (or cracking of bio-oil) occurs over the same length of the freeboard region. This is supported by the feeding point at point-4 which has a shorter length of the freeboard region and it is observed that the yield of the bio-gas dropped drastically. Hence, a shorter freeboard region may bring about a reduction in the bio-gas yield. The feeding point shows very little effect on the char yield and this suggested that char yield is independent of the retainment of biomass in the FBR. It is possible to presume that increasing the height of the FBR may improve the bio-oil yield without having an increment in the char yield.

Table 6. Product yield and temperature at different feeding points for pure cellulose.

Location	Product Yield (%)			Outlet Temperature(K)
	Bio-oil	Bio-gas	Char	
Point-1	87.98	15.33	1.77	790.90
Point-2	87.06	14.54	1.78	787.30
Point-3	81.86	16.51	1.69	775.46
Point-4	37.64	2.85	1.36	761.09

As for the reactor outlet temperature, it decreases from point-1 to point-4. It is observed that the trend in the variation of reactor outlet temperature with feeding points is proportionally to the trend in the variation of bio-oil yield. This suggests that the bio-oil yield affect the reactor outlet temperature. As the component of the reactor outlet consist of bio-oil, bio-gas, char and nitrogen, the decrement in the organic material actually reduces the temperature of the reactor. Applying the conservation of energy, given that the specific heat capacity of each material remains constant, as the mass flowrate of the nitrogen increases or the mass flowrate of the organic material decreases, the temperature of the reactor will decrease with the same amount of energy conserved [31]. In conclusion, the feeding point of pure cellulose is at the optimal at the dense bed zone. However, a further

study at the splash zone could be conducted by giving the biomass the equal residence time if fed in the dense bed zone by lowering the fluidizing velocity.

4.2. Red oak

With the model developed for the study of feeding point for pure cellulose feedstock, the same model was employed to different biomass feedstocks in order to study the effect of feeding points for different biomass. The validation of red oak simulation has provided the author with the confidence to use red oak as the second biomass feedstock in the feeding point study. Table 7 shows the collection of simulation results from the pyrolysis of red oak at different feeding points. The presence of hemicellulose and lignin may strongly influence the feeding point results.

Table 7. Product yield and temperature at different feeding points for red oak.

Location	Product Yield (%)			Outlet Temperature(K)
	Bio-oil	Bio-gas	Char	
Point-1	75.18	23.31	9.00	782.45
Point-2	83.75	14.57	8.04	781.27
Point-3	87.80	11.21	7.48	774.80
Point-4	35.15	6.86	8.34	749.96

Since all the biomass components have a constant kinetic reaction and physical properties, it's safe to assume that the feeding point affects the product yields directly. With constant fluidizing velocity, feeding point affects the residence time of the volatile components. From Table 7, the yield of the bio-oil increases from point-1 to point-3. This shows that the presence of lignin and hemicellulose has affected the influence of the feeding point on the bio-oil yield. It can be concluded that the red oak can be fed on the splash zone to obtain high bio-oil yield. In the aspect of bio-gas yield, the trend for red oak feedstock is decreasing. The amount of bio-gas decreases as the feeding of biomass change from the dense bed to the splash zone suggests that the biomass components stills depend heavily on the fluidizing bed length to have sufficient residence time. Since hemicellulose has the tendency to produce more bio-gas, hemicellulose component has less residence time to produce the bio-gas when the feed point shift from dense bed to the splash zone.

As for the char yield, it is in an agreement with the result from the feeding point study of pure cellulose. Hence, the char yield can be regarded as an independent variable of the feeding point. However, the exact result may vary with the type of biomass [4]. The reactor outlet temperature shows a decreasing trend as the feeding point approaches towards the reactor outlet. This is consistent with the results from the feeding point study of pure cellulose regarding the reactor outlet temperature because the decreasing trend of organic material at the outlet reduces the outlet temperature. However, it should also be noted that the presence of hemicellulose and lignin will also affect the influence of feeding point to an extent [30, 32]. In conclusion, the optimum feeding point for red oak

feedstock is at the splash zone of the FBR with high bio-oil yield, low bio-gas and char yield, and optimum reactor temperature.

5. Conclusions

The pyrolysis process in fluidized bed is affected by parameters such as temperature, particle size, biomass, feeding point and fluidizing velocity; hence, optimization of the reactor design requires careful and detailed considerations. From the literature review, it is discovered that there is a lack of research study on the feeding point of biomass on pyrolysis in fluidized bed reactor. This study is crucial as with different biomass, the feeding point of the biomass in the fluidized bed reactor will affect the heat transfer and the residence time, which ultimately affect the product yields. An experimental paper by Xue et al. (2012) is selected to validate the simulated CFD model with literature support. An extensive literature has also been reviewed to select the most suitable chemical kinetic model and physical models (especially multiphase model and viscous model) for this study. The chemical kinetic model selected is the global kinetic scheme for cellulose superimposes on the hemicellulose and lignin. The physical models selected are Eulerian model for the multiphase model and laminar model as the viscous model.

With the confidence in the validated model, the parametric study proceeds. The parametric study is also conducted on the two different biomass feedstocks used in the validation run. In the feeding point study in pure cellulose, it is suggested that the optimum feeding point is at the dense bed zone, which gives the highest bio-oil yield. However, for the red oak feedstock, the optimum feeding point is on the splash zone with the highest bio-oil yield and low bio-gas yield. It is presumed that the different biomass components will affect the influence of feeding point leading to different results with varying biomass feedstocks. It is also observed that the char yield is independent of the feeding point. The future work would focus on conducting experiments to confirm the simulation result. With the verification from the experiment on the feeding point study, different biomass feedstock can be studied to optimize its respective feeding point.

There is room for improvement in the validation of the model. Since the bio-gas is assumed to consist only of methane, an average physical property of a bio-gas produced in the same pyrolysis temperature could be used to improve the accuracy of the model. Another approach to improve on the accuracy of the validated model is to assign different physical properties for each different biomass components. Hence, a deeper study of the biomass components needs to be conducted to study the physical property of each component.

References

1. Basu, P. (2010). *Biomass gasification and pyrolysis: Practical design and theory*. UK: Academic Press.
2. Shaddix, C.; and Hardesty, D. (1999). *Combustion properties of biomass flash pyrolysis oils*. Combustion Research Facility, Sandia National Laboratories, Livermore, CA.

3. Mohan, D.; Pittman-Jr., C.; and Steele, P. (2006). Pyrolysis of wood/biomass for bio-oil: a critical review. *Energy & Fuels*, 20, 848-889.
4. D. Scott and J. Piskorz. (1984). The continuous flash pyrolysis of biomass. *The Canadian Journal of Chemical Engineering*, 62, 404-412.
5. M. Stammbach, B. Kraaz, R. Hagenbucher and W. Richarz. (1989). "Pyrolysis of sewage sludge in a fluidized bed. *Energy Fuels*, 3, 255-259.
6. D. Scott, P. Majerski, J. Piskorz and D. Radlein. (1999). A second look of fast pyrolysis of biomass - the RTI process. *Journal of Analytical and Applied Pyrolysis*, 51, 23-37.
7. D. Neogi, C. Chang and W. Walawender. (1986). Study of coal gasification in an experimental fluidized bed reactor. *AIChE Journal*, 32, 17.
8. Q. Xue, D. Dalluge, T. Heindel, R. Fox and R. Brown. (2012). Experimental validation and CFD modeling study of biomass fast pyrolysis in fludized-bed reactors. *Fuel*, 97, 757-769.
9. H. Versteeg and W. Malalasekera. (2007). *An introduction to computational fluid dynamics: The finite volume method*. (2nd ed.). England: Pearson Education Limited.
10. K. Papadikis, S. Gu, A. Bridgwater and H. Gerhauser. (2009). Application of CF to model fast pyrolysis of biomass. *Fuel Processing Technology*, 90, 504-512.
11. J. Anderson. (1995). *Computational Fluid Dynamics: The basics with applications*. USA: McGraw-Hill, 1995.
12. R. Fox. (2006). CFD models for analysis and design of chemical reactors. *Advances in Chemical Engineering*, 231-305.
13. S. Rapagna and G. Celso. (2008). Devolatilizaion of wood particles in a hot fluidized bed: product yields and conversion rates. *Biomass and Bioenergy*, 32, 1123-1129.
14. D. Lathouwers and J. Bellan (2001). Modeling of dense gas-solid reactive mixture applied to biomass pyrolysis in a fluidized bed. *International Journal of Multiphase Flow*, 27, 2155-2187.
15. ANSYS®, (2011). Fluent User's Guide 14.0. USA: ANSYS Inc.
16. K. Papadikis, A. Bridgwater and S. Gu (2008). CFD modelling of the fast pyrolysis of biomass in fluidised bed reactors, Part A: Eulerian. *Chemical Engineering Science*, 63, 4218-4227.
17. P. Mellin, Q. Zhang, E. Kantarelis and W. Yang, (2013). An Euler-Euler approach to modeling biomass fast pyrolysis in fluidized-bed reactors - Focusing on the gas phase. *Applied Thermal Engineering*, 58, 344-353.
18. R. Singh, A. Brink and M. Hupa (2013). CFD modeling to study fluidized bed combustion and gasification. *Applied Thermal Engineering*, 52, 585-614.
19. J. Kuipers, W. Prins and W. Swaaij. (1992). Numerical calculation of wall-to-bed heat transfer. *AIChe Journal*, 38, 7.
20. C. Loha, H. Chattopadhyay and P. Chatterjee (2012). Assessment of drag models in simulating bubbling fluidized bed hydrodynamics. *Chemical Engineering Science*, 75, 400-407.

21. M. Hamidipour, J. Chen and F. Larachi. (2012). CFD study on hydrodynamics in three-phase fluidized beds - Application of turbulence models and experimental validation. *Chemical Engineering Science*, 78, 167-180.
22. J. White, W. Catallo and B. Legendre. (2011). Biomass pyrolysis kinetics: A comparative critical review with relevant agricultural residue case studies. *Journal of Analytical and Applied Pyrolysis*, 91, 1-33.
23. A. Bradbury, Y. Sakai and F. Shafizadeh. (1979). A kinetic model for pyrolysis of cellulose. *Journal of Applied Polymer Science*, 23, 3271-3280.
24. F. Shafizadeh. (1982). Introduction to pyrolysis of biomass. *Journal of Analytical and Applied Pyrolysis*, 3, 283-305.
25. F. Shafizadeh and A. Bradbury. (1979). Thermal degradation of cellulose in air and nitrogen at low temperature. *Journal of Applied Polymer Science*, 23, 1432-1444.
26. R. Miller and J. Bellan. (1997). A generalized biomass pyrolysis model based on superimposed cellulose, hemicellulose, and lignin kinetics. *Combustion Science and Technology*, 126, 97-138.
27. A. Liden, F. Berruti and D. Scott. (1988). A kinetic model for the production of liquids from the flash pyrolysis of biomass. *Chemical Engineering Community*, 65, 207-221.
28. T. Iman and S. Capareda. (2012). Characterization of bio-oil, syn-gas, and bio-char from switchgrass pyrolysis at various temperature. *Journal of Analytical and Applied Pyrolysis*, 93, 170-177.
29. C. Couhert, J.-M. Commandre and S. Salvador. (2009). Is it possible to predict gas yields of any biomass after rapid pyrolysis at high temperature from its composition in cellulose, hemicellulose and lignin? *Fuel*, 88, 408-417, 2009.
30. G. Dorez, L. Ferry, R. Sonnier, A. Taguet and J.-M. Lopez-Cuesta. (2014). Effect of cellulose, hemicellulose and lignin contents on pyrolysis and combustion of natural fibers. *Journal of Analytical and Applied Pyrolysis*, 107, 323-331.
31. J. Corella, J. Herguido and F. Alday. (1988). Pyrolysis and steam gasification in fluidized beds. Influence of the type and location of the biomass feeding point on the product distribution. *Elsevier Applied Science*, 384-398.
32. T. Hosoya, H. Kawamoto and S. Saka. (2007). Cellulose-hemicellulose and cellulose-lignin interactions in wood pyrolysis at gasification temperature. *Journal of Analytic and Applied Pyrolysis*, 80, 118-125.
33. C. Hamelinck and A. Faaij. (2006). Outlook for advanced biofuels. *Energy Policy*, 34, 3268-3283.